COMMUN. MATH. SCI.
Vol. 14, No. 3, pp. 683–704

A NUMERICAL METHOD FOR THE COMPUTATION OF TANGENT VECTORS TO 2×2 HYPERBOLIC SYSTEMS OF CONSERVATION LAWS*

MICHAEL HERTY† AND BENEDETTO PICCOLI‡

Abstract. We are interested in the development of a numerical method for solving optimal control problems governed by hyperbolic systems of conservation laws. The main difficulty of computing the derivative in the case of shock waves is resolved in the presented scheme. Our approach is based on a combination of a relaxation approach in combination with a numerical scheme to resolve the evolution of the tangent vectors. Numerical results for optimal control problems are presented.

Key words. Conservation laws, optimization, tangent vectors.

AMS subject classifications. 35L65, 49K20, 49K40.

1. Introduction

We are concerned with a numerical approach to optimization problems governed by systems of hyperbolic partial differential equations in a single spatial dimension. As a prototype, we consider a tracking type problem for a terminal state y_d prescribed at some given time $t=T$ where the control acts as initial condition u_0. A mathematical formulation of this optimal control problem is reduced to minimizing a functional, and, for instance, it can be stated as follows:

$$\min_{u_0} J(y,y_d), \tag{1.1}$$

where J is the given cost functional and $y\in\mathbb{R}^n$ is the unique entropy solution of the nonlinear conservation law

$$\begin{aligned} y_t+f(y)_x&=0, && x\in\mathbb{R}, \quad t>0,\\ y(0,x)&=u_0(x), && x\in\mathbb{R}. \end{aligned} \tag{1.2}$$

There has been tremendous progress in both analytical and numerical studies of problems of type (1.1) and (1.2); see [1–3, 7, 8, 12, 13, 18–20, 22, 24, 27–29]. Its solution relies on the property of the evolution operator $\mathcal{S}_t : u_0(\cdot)\to y(\cdot,t)=\mathcal{S}_t u_0(\cdot)$ for (1.2). It is known that the semi-group $\mathcal{S}_t$ generated by a nonlinear hyperbolic conservation law is generically nondifferentiable in L^1 even in the scalar one-dimensional (1D) case (see, e.g., [12, Example 1]). A calculus for the first-order variations of $\mathcal{S}_t u_0$ with respect to u_0 has been established in [12, theorems 2.2 and 2.3] for general 1D systems of conservation laws with a piecewise Lipschitz continuous u_0 that contains finitely many discontinuities. Therein, the concept of generalized first-order tangent vectors has been introduced to characterize the evolution of variations with respect to u_0; see [12, equations (2.16)–(2.18)]. It has been further extended in [11] to establish continuous dependence of $\mathcal{S}_t$ on the initial data u_0. This result has been extended to BV initial data in [3, 7] and lead to the introduction of a differential structure for $u_0\to\mathcal{S}_t u_0$ called shift-differentiability;

*Received: May 4, 2014; accepted (in revised form): April 18, 2015. Communicated by Lorenzo Pareschi.

†RWTH Aachen University, IGPM, Templergraben 55, 52056 Aachen, Germany (herty@igpm.rwth-aachen.de).

‡Department of Mathematics, Rutgers University, Camden, NJ, 08102, USA (piccoli@camden.rutgers.edu).

see [3, Definition 5.1]. Further extensions have also been discussed, for example [17]. Related to that, equations for the generalized cotangent vectors have been introduced for 1D systems in [9, Proposition 4]. These equations (also called adjoint equations) consist of a nonconservative transport equation [9, Equation (4.2)] and an ordinary differential equation [9, equations (4.3)–(4.5)] for the tangent vector and shift in the positions of possible shocks in $y(x,t)$, respectively. Necessary conditions for a general optimal control problem have been established in [9, Theorem 1]. However, this result was obtained using strong assumptions on u_0 (see [9, Remark 4] and [3, Example 5.5]), which in the 1D scalar case can be relaxed as shown in [13, 29]. We note that the nonconservative transport part of the adjoint equation has been intensively studied also independently from the optimal control context. In the scalar case, we refer to [5,6,26,29] for a notion of solutions and properties of solutions to those equations. Analytical results for optimal control problems in the case of a scalar hyperbolic conservation law with a convex flux have also been developed using a different approach in [29]. The relation to the weak formulation has been discussed in [2] in the case of Burgers' equation.

Numerical methods for the optimal control problems have been discussed in [1, 20]. In [19], the adjoint equation has been discretized using a Lax–Friedrichs-type scheme, obtained by including conditions along shocks and modifying the Lax–Friedrichs numerical viscosity. Convergence of the modified Lax–Friedrichs scheme has been rigorously proved in the case of a smooth convex flux function. Convergence results have also been obtained in [29] for the class of schemes satisfying the one-sided Lipschitz condition (OSLC) and in [1] for implicit-explicit finite-volume methods. Other examples of finite volume methods and Lagrangian methods are given in [14, 23].

In [13], analytical and numerical results for the optimal control problem (1.1) coupled with the 1D inviscid Burgers' equation have been presented in the particular case of a least-square cost functional J. Therein, existence of a minimizer u_0 was proven, but uniqueness could not be obtained for discontinuous functions y. This result was also extended to the discretized optimization problem provided that the numerical schemes satisfy either the OSLC or discrete Oleinik's entropy condition. Furthermore, convergence of numerical schemes was investigated in the case of convex flux functions and with a priori known shock positions, and numerical resolution of the adjoint equations in both the smooth and non-smooth cases was studied. In [21] perturbations of initial data are studied using an additional spatial dimension. Numerical results as well as a formalism to derive the linearized equations have been presented therein. The scalar case of a production model coupled to ordinary differential equations has been studied in [16]. Therein, convergence of the wave-front tracking approximation to the tangent vector equation is proven.

We contribute to the discussion by introducing a novel scheme which allows us to include the arising discontinuities in an optimization framework and *without* an a priori assumption on the location of the discontinuities. This is possible and computationally efficient under three basic assumptions: first, we only compute derivatives with respect to piecewise constant controls u_0; second, the system (1.2) is not solved directly, but an ϵ-relaxation approximation (2.2) is solved instead and last, we compute the exact derivative for the ϵ-approximation of the system (2.2) using tangent vectors. The number of discontinuities in u_0 may herein be as large as $\frac{1}{\Delta x}$, where Δx is the spatial width of the numerical grid. The overall algorithm requires the solution of two additional hyperbolic partial differential equations. The motivation and theoretical investigations are presented in Section 2 and numerical results in Section 3. The results presented are on the relaxation formulation of the Burgers' equation as well as linear hyperbolic sys-

tems. Nevertheless, the approach also applies to nonlinear hyperbolic systems. In this case, the current approach leads to higher diffusion due to the requirement of a single characteristic speed bounding all characteristic speed, as seen in the implementation for example in equation (2.25).

2. Motivation and theoretical results

In order to derive a numerical scheme, we consider a relaxation approximation [25] to (1.2). For simplicity, we consider only the Jin–Xin relaxation in the case $n=1$ and on the full real line $x\in\mathbb{R}$. Then the hyperbolic relaxation for

$$y_t^{(1)} + f(y^{(1)})_x = 0,\ y^{(1)}(0,x) = u_0(x), \tag{2.1}$$

is given by

$$y_t + \begin{pmatrix} 0 & 1 \\ a^2 & 0 \end{pmatrix} y_x = \begin{pmatrix} 0 \\ \frac{1}{\epsilon}(f(y^{(1)}) - y^{(2)}) \end{pmatrix} \tag{2.2}$$

and by the initial data

$$y^{(1)}(0,x) = u_0(x),\ y^{(2)}(0,x) = f(u_0(x)). \tag{2.3}$$

We assume that the value a^2 fulfills the subcharacteristic condition

$$a^2 - f'(y^{(1)})^2 \geq 0 \forall y^{(1)}. \tag{2.4}$$

For positive ϵ, it is known that a solution y yields an approximation to (1.2) in the following sense. For ϵ sufficiently small, we have up to second order in ϵ

$$y_t^{(1)} + f(y^{(1)})_x = \epsilon \left(\left(a^2 - f'(y^{(1)})^2 \right) y_x^{(1)} \right)_x.$$

Formally we obtain the original conservation law for $y^{(1)}$ in the limit $\epsilon = 0$. We refer to [4] for a detailed analysis. For $\epsilon > 0$ the method is known as a relaxing scheme. The main advantage of (2.2) over (1.2) is the linear transport which greatly simplifies the computation of associated tangent vectors (in particular the numerical resolution of the shock variations will turn out trivial for (2.2)).

In the following, we will therefore discuss the optimization problem (1.1) with respect to (2.2). Still, the numerical computation of tangent vectors in general poses severe challenges addressed below. Therefore, we further simplify by only considering piecewise constant controls u_0. In the following, $TV(\cdot)$ denotes the total variation.

Given some $C > 0$, we consider problem (1.1) subject to (2.2) and (2.3) for controls $u_0 \in \mathcal{U}$.

Definition 2.1. *We indicate by* $\mathcal{U} := \{u : \mathbb{R} \to \mathbb{R} : u$ *measurable,* $TV(u) \leq C$, u *piecewise constant*$\}$ *the set of admissible controls. For every* $u \in \mathcal{U}$, *we indicate by* $x_k = x_k(u), k = 1, \dots, N(u)$ *the points of discontinuity of* u.

For $y_d \in L^1(\mathbb{R})$, some $T > 0$, and a bounded interval $I \subset \mathbb{R}$, we consider as a prototype example an unregularized cost functional of tracking type

$$J(y, y_d; T, I) = \int \chi_I(x) \left(y^{(1)}(T,x) - y_d(x) \right)^2 dx. \tag{2.5}$$

The dependence of J on terminal time T and the interval I will be dropped from now on. We assume that both are fixed and will not change throughout the manuscript.

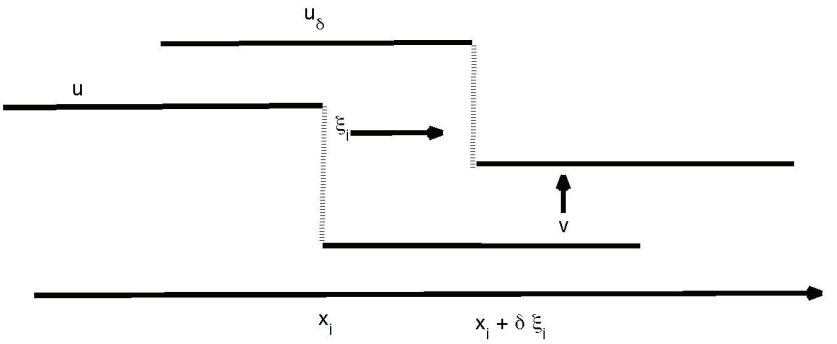

FIG. 2.1. *Construction of a tangent vector* (ξ_i, v) *to* u_δ *having a discontinuity at* x_i.

We now introduce the notion of tangent vectors; see [12] and [11]. In (2.2), we assume $\epsilon > 0$ fixed, $f \in C^4(\mathbb{R})$, and a^2 fulfills the subcharacteristic condition. For a function $u \in \mathcal{U}$ a generalized tangent vector consists of two components (v, ξ), where $v \in L^1(\mathbb{R})$ describes the L^1 infinitesimal displacement and $\xi \in \mathbb{R}^{N(u)}$ describes the infinitesimal displacement of $N(u)$ discontinuities. A norm on the space of tangent vectors $T_u := L^1(\mathbb{R}; \mathbb{R}^n) \times \mathbb{R}^{N(u)}$ is given by

$$\|(v, \xi)\| := \|v\|_{L^1} + \sum_{i=1}^{N(u)} |\Delta_i u| \, |\xi_i|, \tag{2.6}$$

where $\Delta_i u = u(x_i+) - u(x_i-)$ denotes the jump in u. The norm depends on u through the number of points of discontinuity. Tangent vectors may be used to describe variations of u, as exemplified in Figure 2.1. For $\delta > 0$, an infinitesimal displacement u_δ of u is given by

$$u_\delta = u + \delta v - \sum_{i:\xi_i > 0}^{N(u)} \Delta_i u \, \chi_{[x_i, x_i + \delta\xi_i]} + \sum_{i:\xi_i < 0}^{N(u)} \Delta_i u \, \chi_{[x_i + \delta\xi_i, x_i]}. \tag{2.7}$$

u_δ is obtained from u by shifting the function values by δv and the ith discontinuity by $\delta\xi_i$. For δ sufficiently small u_δ has the same number of discontinuities as u. Note that, if $\xi \neq 0$, then the function $\delta \to u_\delta$ is *not* differentiable in L^1, as the ratio $\frac{u_{\delta+h} - u_\delta}{h}$ does not converge to any limit in L^1 for $h \to 0$. However, the previous limit remains meaningful if interpreted as a weak limit in a space of measures with a singular point mass located at x_i and having magnitude $|\Delta_i u| \xi_i$. Therefore, in [12], a class of variations $\delta \to u_\delta$ is described up to first order by (generalized) tangent vectors (v, ξ).

In general, the norm (2.6) depends on the number of discontinuities $N(u)$ and therefore on u. As a numerical method, we will restrict ourselves to piecewise constant controls u_0. We are going study the number $N(u_0)$ equal to the number of grid cells in the spatial domain. This number is known a priori.

We introduce some notation and definitions (see [11, 12]) already in view of the special system (2.2). Let $u \in L^1(\mathbb{R}; \mathbb{R}^n)$ be a piecewise Lipschitz continuous function with $N = N(u)$ jumps. Consider Σ_u the family of all continuous paths $\gamma : [0, \delta_0] \to L^1_{loc}$

with $\gamma(0)=u$ with δ_0 possibly depending on γ. We recall the following definition [12, Definition 1.3].

DEFINITION 2.2. *The space of generalized tangent vectors to a piecewise Lipschitz function u with jumps at the points $x_1<x_2\cdots<x_N$ is $T_u:=L^1(\mathbb{R};\mathbb{R}^n)\times\mathbb{R}^N$. A continuous path $\gamma\in\Sigma_u$ generates a tangent vector $(v,\xi)\in T_u$ if*

$$\lim_{\delta\to 0}\frac{1}{\delta}\|\gamma(\delta)-\bar\gamma(\delta)\|_{L^1}=0$$

for

$$\bar\gamma:=u+\delta v-\sum_{i:\xi_i>0}\Delta_i u\,\chi_{[x_i,x_i+\delta\xi_i]}+\sum_{i:\xi_i<0}\Delta_i u\,\chi_{[x_i+\delta\xi_i,x_i]}.$$

Let u be a piecewise Lipschitz function with simple discontinuities [12, Definition 2]. Then, a path $\gamma\in\Sigma_u$ is a regular variation for u if additionally all function $\gamma(\delta)=u_\delta$ are piecewise Lipschitz with simple discontinuities and the jumps x_i^δ depend continuously on δ.

A regular variation γ for u generates a tangent vector (v,ξ) by

$$\xi_i=\lim_{\delta\to 0}\frac{x_i^\delta-x_i}{\delta},\ \lim_{\delta\to 0}\int_a^b\|\frac{u^\delta(x_i^\delta+y)-u(x_i+y)}{\delta}-v(x_i+y)-\xi_i u_x(x_i+y)\|dy=0 \quad (2.8)$$

whenever $[x_i+a,x_i+b]$ does not contain any other point of discontinuity of u except x_i. Further, the length of a regular path γ can be computed by (2.6). We now consider the initial data u_0 and a regular variation generating the tangent vector $(v,\xi)\in T_u$. Under suitable regularity assumptions [12, Theorem 2.2], regular variations are locally preserved by system (2.2), and linearized equations for the time evolution of the tangent vector $(v(t,\cdot),\xi(\cdot))$ can be derived. We have the following result [12, Theorem 2.2].

LEMMA 2.1. *Let $y(\cdot,\cdot)$ be a piecewise Lipschitz continuous solution to* (2.2) *and initial data* (2.3) *$y(0,\cdot)=\bar y$ piecewise Lipschitz with N simple discontinuities. Let $(\bar v,\bar\xi)\in T_{\bar y}$ be a tangent vector to $\bar y$ generated by the regular variation γ with $\gamma(\delta)=\bar y_\delta$. Let $y_\delta(t,x)$ be the solution to* (2.2) *and initial data* (2.3) *$y_\delta(0,x)=\bar y_\delta(\cdot)$. Then there exists a time $t_0>0$ such that, for all $t\in[0,t_0]$, the path $\bar\gamma$ with $\bar\gamma(\delta)=y_\delta(t,\cdot)$ is a regular variation of $y(t,\cdot)$ generating the tangent vector $(v(t),\xi(t))\in T_{y(t,\cdot)}$. Further, (v,ξ) is the unique broad solution to*

$$v(0,\cdot)=\bar v(\cdot),\quad v_t+\begin{pmatrix}0&1\\a^2&0\end{pmatrix}v_x=\frac{1}{\epsilon}\begin{pmatrix}0\\f'(y^{(1)})v^{(1)}-v^{(2)}\end{pmatrix}, \quad (2.9)$$

where $v=(v^{(1)},v^{(2)})$ and outside of the discontinuities of y. For $i=1,\dots,N$ we have

$$\xi_i(t)=\bar\xi_i \text{ and } l_j\cdot(\Delta_i v+\Delta_i y_x\,\xi_i)=0\, j\neq k_i. \quad (2.10)$$

along each line of discontinuity $x_i(t)$ where y has a discontinuity in the k_ith characteristic family. Here, $\Delta_i v=v(x_i(t)+,t)-v(x_i(t)-,t)$, and l_j denotes the jth left eigenvector of the matrix $\begin{pmatrix}0&1\\a^2&0\end{pmatrix}$.

The proof of Lemma 2.1 follows from Theorem 2.2 [8], which has been repeated in Appendix A for convenience. We observe that system (2.2) fulfills the hypothesis

(H1) to (H3) due to its linearity in the flux and since $f \in C^4$. The hypotheses are also detailed in Appendix A. Due to the linearity of the hyperbolic flux, the eigenvectors and eigenvalues are independent of y. Therefore, the shock sensitivities ξ_i are constant in time, leading to equation (2.10). The evolution equation for v strongly simplifies, as well, leading to equation (2.9). According to [12, Definition 2] $\bar{u} \in \mathcal{U}$ and $\bar{y} = (\bar{u}, f(\bar{u}))$ are piecewise Lipschitz with simple discontinuities. The equations (2.9) and (2.10) are particularly simple due to the linear transport in the hyperbolic relaxation. In particular, the equation for ξ_i is solved without any effort, since ξ_i is constant in time. Further, if we diagonalize (2.2) first and then apply the tangent vector calculus, the second equation (2.10) simplifies. We come back to this point later in the numerical scheme. It is important to note that in the previous result it is assumed that all variations u_δ (resp. y_δ) posses the same number of discontinuities which in the case of problem (1.1) is unknown a priori. An interpretation of the second condition of equation (2.10) may be as follows: given a discontinuity in family i, the condition prevents a discontinuity at the same position in another family $j \neq i$.

Tangent vectors and their property (2.8) can be used to compute the variations of the cost functional (2.5).

LEMMA 2.3. *Assume the assertions of Lemma 2.1 hold. Assume that $t_0 > T$. Let J be given by* (2.5)*, and assume I is sufficiently large. Then, the variation of J with respect to a tangent vector (v,ξ) for initial data $y(0,x) = (u_0(x), f(u_0(x)))$ is given by*

$$\begin{aligned}
&\Delta_{(v,\xi)} J(y, y_d) \\
=&2 \int \chi_I(x) \left(y^{(1)}(T,x) - y_d(x) \right) v^{(1)}(T,x) dx \\
&+ \sum_{i=1}^{N(u_0)} \left(\left(y^{(1)}(T, x_i+) - y_d(x_i+) \right) + \left(y^{(1)}(T, x_i-) - y_d(x_i-) \right) \right) \Delta_i y^{(1)}(T,\cdot) \xi_i(T).
\end{aligned} \tag{2.11}$$

In other words, calling $\gamma(\delta)$ a curve generating the tangent vector (v,ξ) and y_δ the solution for initial datum $\gamma(\delta)$, we have

$$J(y_\delta, y_d) = J(y, y_d) + \delta \ \Delta_{(v,\xi)} J(y, y_d) + o(\delta). \tag{2.12}$$

Note that the summation is on the discontinuities of $y^{(1)}$ at terminal time T related by Lemma 2.1 to the number of discontinuities of u_0 (resp. y_0) reflecting the original problem. The proof is similar to [16, Proposition 1] and is omitted.

Lemma 2.3 and equation (2.7) already suggest a numerical method for solving (1.1) with cost functional (2.5). Given some control u_0 and a stepsize $\rho > 0$, we obtain a new control $\tilde{u}_0$ corresponding to the smaller value of the cost functional J by the following variation

$$\tilde{u}_0(x) = u_0(x) - \left(\rho v(0,x) - \sum_{i:\xi_i(0)>0}^{N(u_0)} \Delta_i u_0 \, \chi_{[x_i, x_i + \rho \xi_i(0)]} + \sum_{i:\xi_i(0)<0}^{N(u_0)} \Delta_i u_0 \, \chi_{[x_i + \rho \xi_i(0), x_i]} \right), \tag{2.13}$$

and $\tilde{y}_0 = (\tilde{u}_0, f(\tilde{u}_0))$. Further, $v(0,x)$ is the solution at time $t = 0$ to (2.9) for *terminal* data

$$v^{(1)}(T,x) = \left(y_d(x) - y^{(1)}(T,x) \right), \ v^{(2)}(T,x) = 0, \tag{2.14}$$

and $\xi_i(0)$ the solution to (2.10) with *terminal* data

$$\xi_i(T) = \Big(\Big(y_d(x_i+) - y^{(1)}(T,x_i+)\Big) + \Big(y_d(x_i-) - y^{(1)}(T,x_i-)\Big)\Big)\,\Delta_i y^{(1)}(T). \tag{2.15}$$

Now, the given choice for $(v(T,x),\xi(T))$ yields:

$$\begin{aligned}
&\Delta_{(v,\xi)} J(y,y_d)\\
&= -2\int \chi_I(x)\Big(y^{(1)}(T,x) - y_d(x)\Big)^2 dx\\
&\quad - \sum_{i=1}^{N(u_0)} \Big(\Big(y^{(1)}(T,x_i+) - y_d(x_i+)\Big) + \Big(y^{(1)}(T,x_i-) - y_d(x_i-)\Big)\Big)^2 \Big(\Delta_i y^{(1)}(T,\cdot)\Big)^2.
\end{aligned}$$

Denote by $\tilde{y}$ the solution to equation (2.2) with initial data $\tilde{y}_0 = (\tilde{u}_0, f(\tilde{u}_0))$. The solution to initial data $(u_0, f(u_0))$ is denoted by y. Then, according to (2.12) we obtain

$$J(\tilde{y},y_d) < J(y,y_d) \tag{2.16}$$

for ρ sufficiently small.

Note that this requires us to solve (2.9) backwards in time and to fulfill (2.10). The previous computations motivate a numerical scheme for approximately solving (1.1), (2.2), and (2.5).

Before stating the full discrete algorithm, we reformulate and comment on some parts of the method. System (2.2) is diagonalisable with eigenvalues $\lambda_{1,2} = \pm a$ and characteristic variables

$$\eta^{(1)} = y^{(2)} + a y^{(1)} \text{ and } \eta^{(2)} = y^{(2)} - a y^{(1)}. \tag{2.17}$$

Also, in view of condition (2.10), it is numerically advantageous to consider the minimization problem for J in characteristic variables $\eta = (\eta^{(1)}, \eta^{(2)})$. Furthermore, in view of (2.13) equation, (2.9) will be solved backwards in time for given terminal data $v(T,x)$. We obtain for $\tilde{v}(t,x) = v(T-t,x)$ the system

$$\tilde{v}(0,\cdot) = v(T,\cdot),\ \tilde{v}_t - \begin{pmatrix} 0 & 1 \\ a^2 & 0 \end{pmatrix} \tilde{v}_x = \frac{1}{\epsilon}\begin{pmatrix} 0 \\ \tilde{v}^{(2)} - f'(y^{(1)}(T-t,\cdot))\tilde{v}^{(1)} \end{pmatrix}. \tag{2.18}$$

and eigenvalues $\lambda_{1,2} = \mp a$ and corresponding characteristic variables

$$\varphi^{(1)} = \tilde{v}^{(2)} + a\tilde{v}^{(1)} \text{ and } \varphi^{(2)} = \tilde{v}^{(2)} - a\tilde{v}^{(1)}.$$

Let $I = [0,1]$, $T > 0$, y_d and $\epsilon > 0$ be given. The cost functional J is given by equation (2.5). We discuss the numerical discretization of problem (2.19) using a first-order finite-volume scheme with periodic boundary conditions. Note that we leave (for the moment) *both* components of the initial data y_0 subject to optimization.

$$\min_{y_0 = (y_0^{(1)}, y_0^{(2)})} J \text{ sbj to } (2.2),\ y(0,x) = y_0(x),\ y(t,1) = y(t,0),\ x \in I,\ t \geq 0. \tag{2.19}$$

Fix a^2 such that the subcharacteristic condition (2.4) is fulfilled. Introduce an equidistant spatial grid $\{x_i\}_{i=0}^{N_x}$ on I with $\Delta x = x_{i+1} - x_i$. We choose Δt such that the CFL condition holds (i.e., $\Delta t|a| = \Delta x$) and denote by $t^n = \Delta t\, n$ for $n = 0,\ldots,N_t$. We write $x_{i+\frac{1}{2}} = x_i + \frac{\Delta x}{2}$ and, for simplicity, assume $x_{N_x} = 1$ and $t^{N_t} = T$. Also for notational

convenience we denote by $x_{-\frac{1}{2}} = x_{N_x-\frac{1}{2}}$ and $x_{N_x+\frac{1}{2}} = x_{\frac{1}{2}}$. Let $\mathcal{T}^{-1} \in \mathbb{R}^{2\times 2}$ be the transformation to characteristic variables (2.17), i.e.,

$$\mathcal{T}^{-1} \begin{pmatrix} 0 & 1 \\ a^2 & 0 \end{pmatrix} \mathcal{T} = \begin{pmatrix} a & 0 \\ 0 & -a \end{pmatrix} \text{ and } \eta = \mathcal{T}^{-1} y.$$

On a time interval $[t^n, t^{n+1}]$, we may introduce an operator splitting [25] to discretize source and transport term. In characteristic variables, the splitting for $t \in [t^n, t^{n+1}]$ reads

$$\begin{aligned}
&\partial_t \eta^{(1)} + a\partial_x \eta^{(1)} = 0, \partial_t \eta^{(2)} = 0, \\
&\partial_t \eta^{(1)} = S(\eta^{(1)}, \eta^{(2)}), \partial_t \eta^{(2)} = S(\eta^{(1)}, \eta^{(2)}), \\
&\partial_t \eta^{(2)} - a\partial_x \eta^{(2)} = 0, \partial_t \eta^{(1)} = 0,
\end{aligned}$$

where $S(\eta^{(1)}, \eta^{(2)}) = \frac{1}{\epsilon}\left(f((\mathcal{T}\eta)^{(1)}) - (\mathcal{T}\eta)^{(2)}\right)$. A discontinuity at time t^n in any component of η_0 therefore moves with speed a and $-a$, respectively. Clearly, we can also express the objective function J in characteristic variables. The corresponding equations are given in Appendix B.

The cell average on $[x_{i-\frac{1}{2}}, x_{i+\frac{1}{2}}]$ at time t^n for any function $u(t,x)$ is denoted by $u_i^n = \frac{1}{\Delta x}\int_{x_{i-\frac{1}{2}}}^{x_{i+\frac{1}{2}}} u(t^n, x)dx$. A first-order Upwind discretization of equation (2.2) using the reformulation in characteristic variables and an exact integration of the source term is given by (2.20) for $i = 0, \dots, N_x$ and $n = 1, \dots, N_t$.

$$y_i^0 = (y_0)_i \tag{2.20a}$$

$$\eta_i^{(1)} = (\mathcal{T}^{-1} y_{i-1}^{n-1})^{(1)}, \eta_0^{(1)} = (\mathcal{T}^{-1} y_{N_x}^{n-1})^{(1)}, \eta_i^{(2)} = (\mathcal{T}^{-1} y_i^{n-1})^{(2)}, \tag{2.20b}$$

$$\tilde{y}_i^{(1)} = (\mathcal{T}\eta_i)^{(1)}, \tilde{y}_i^{(2)} = \exp(-\frac{\Delta t}{\epsilon})(\mathcal{T}\eta_i)^{(2)} + (1 - \exp(-\frac{\Delta t}{\epsilon}))f(\tilde{y}_i^{(1)}), \tag{2.20c}$$

$$\eta_i^{(2)} = (\mathcal{T}^{-1}\tilde{y}_{i+1})^{(2)}, \eta_{N_x}^{(2)} = (\mathcal{T}^{-1}\tilde{y}_0)^{(2)}, \eta_i^{(1)} = (\mathcal{T}^{-1}\tilde{y}_i)^{(1)}, \tag{2.20d}$$

$$y_i^n = \mathcal{T}\eta_i. \tag{2.20e}$$

The discretization (2.20) uses a different splitting compared to [25], which leads to more complicated update formulas above but will be advantageous later on. In the current splitting, we first transport in the first characteristic variable; then we apply the source term; and finally we transport the second characteristic variable. The transformation to characteristic variables η and the CFL condition allows us to resolve the transport exactly. Due to the particular CFL chosen, after one time step, any discontinuity located at a cell interface reaches after Δt again a cell interface $x_{i+\frac{1}{2}}$.

As explained above, instead of equation (2.9), we discretize equation (2.18) to solve for the variations $\tilde{v}$. Similarly to (2.20), we transform (2.18) to characteristic variables φ and resolve the linear transport exactly. If the discretized initial data is denoted by $\tilde{v}_i^0$, then we obtain for $i = 0, \dots, N_x$ and $n = 1, \dots, N_t$.

$$\varphi_i^{(2)} = (\mathcal{T}^{-1}\tilde{v}_{i-1}^{n-1})^{(2)}, \varphi_0^{(2)} = (\mathcal{T}^{-1}\tilde{v}_{N_x}^{n-1})^{(2)}, \varphi_i^{(1)} = (\mathcal{T}^{-1}\tilde{v}_i^{n-1})^{(1)} \tag{2.21a}$$

$$\bar{v}_i^{(1)} = (\mathcal{T}\varphi_i)^{(1)}, \bar{v}_i^{(2)} = \exp(-\frac{\Delta t}{\epsilon})(\mathcal{T}\varphi_i)^{(2)} + (1 - \exp(-\frac{\Delta t}{\epsilon}) f'(y_i^{(1),N_t-n})\bar{v}_i^{(1)} \tag{2.21b}$$

$$\varphi_i^{(1)} = (\mathcal{T}^{-1}\bar{v}_{i+1})^{(1)}, \varphi_{N_x}^{(1)} = (\mathcal{T}^{-1}\bar{v}_0)^{(1)}, \varphi_i^{(2)} = (\mathcal{T}^{-1}\bar{v}_i)^{(2)}, \tag{2.21c}$$

$$\tilde{v}_i^n = \mathcal{T}\varphi_i. \tag{2.21d}$$

Next, we turn to the discretization of equation (2.10). Within a first-order finite volume scheme, a piecewise constant approximation is used to reconstruct the solution, i.e.,

$$y(t,x) \approx \sum_{i=0}^{N_x} \chi_{[t^n,t^{n+1}]\times[x_{i-\frac{1}{2}},x_{i+\frac{1}{2}}]}(t,x) y_i^n, \tag{2.22}$$

and likewise for the initial data. Therefore, numerically solving problem (2.19) naturally leads us to consider piecewise constant controls $y_0 \in \mathcal{U}$ having discontinuities at possibly each cell boundary $x_{i+\frac{1}{2}}$. Therefore, a shift in the position of the discontinuity ξ_i may occur at each boundary $x_{i+\frac{1}{2}}$. As long as the spatial resolution is not modified, the number of discontinuities is however fixed, being a crucial assumption in Theorem 2.1. Since the conservative y and characteristic variables η are equivalent upon the linear transformation $\mathcal{T}$, we optimize in (2.19) for $\eta_0 = \mathcal{T}^{-1} y_0$ instead of y_0.

For fixed N_x, the set of all admissible controls $\mathcal{U}_{ad} \subset \mathcal{U}$ consists of all piecewise constant functions $\eta_0(x)$ given by

$$\eta_0^{(j)}(x) = \sum_{i=0}^{N_x} \chi_{[x_{i-\frac{1}{2}},x_{i+\frac{1}{2}}]}(x) \eta_{0,i}^{(j)}, \; j = 1,2, \tag{2.23}$$

which additionally fulfill

$$(\eta_0^{(1)})_{2i} = (\eta_0^{(1)})_{2i+1}, \, (\eta_0^{(2)})_{2i-1} = (\eta_0^{(2)})_{2i}, \, i = 0, \ldots, \frac{N_x}{2}. \tag{2.24}$$

Note that, for N_x sufficiently large, the condition (2.24) still allows us to approximate any piecewise constant function. The condition (2.24) allows as admissible controls piecewise constant $\eta_0^{(i)} \in \mathcal{U}$ for $i = 1,2$ having each only $\frac{N_x}{2}$ points of discontinuity which are of the following type: the first component $\eta_0^{(1)}$ may have a discontinuity only at $x_{i+\frac{1}{2}}$ for some odd value i, and the second component $\eta_0^{(2)}$ may only have a discontinuity at $x_{i+\frac{1}{2}}$ for some even value i. The construction (2.23) and (2.24) allows that for any given discretization cell i, either the first or the second component has a discontinuity across the cell boundary $i+\frac{1}{2}$. The other component is constant across the cell boundary. This ensures that the second part of condition (2.10) is fulfilled. Further, the jump is parallel to the eigenvectors and does not split under advection. This structure is preserved in the splitting scheme below, and therefore condition (2.10) is automatically fulfilled after transport and application of the source term.

When computing the tangent vector to η_0, we now obtain the L^1-variations φ_0 and the variation in the position of the discontinuities ξ_i. We denote by $\xi_i, i = 0, \ldots, N_x$ the variation of the discontinuity at position $x_{i+\frac{1}{2}}$. Hence, ξ_i for i odd (even) is the variation of the discontinuity in the first (second) component of η_0. In original variables, the equation for ξ_i is given by equation (2.15). Transformation in characteristic variables leads to equation (B.2c), repeated here for convenience:

$$\xi_j(T) = \frac{1}{2}\left(\left(\overline{\Delta}_{i(j)}\eta^{(1),N_t} - \overline{\Delta}_{i(j)}\eta^{(2),N_t} - \overline{\Delta}_{i(j)} y_d\right)\right)\left(\widehat{\Delta}_{i(j)}\eta^{(1),N_t} - \widehat{\Delta}_{i(j)}\eta^{(2),N_t}\right),$$

where $\overline{\Delta} w_k = \frac{1}{2a}(w_{k+1} + w_k)$ and $\widehat{\Delta} w_k = w_{k+1} - w_k$. Here, $i(j)$ denotes the index of the location $x_{i+\frac{1}{2}}$ of the jth discontinuity in the initial data (i.e., for given j, we determine

i such that $x_{i+\frac{1}{2}} = x_{j+\frac{1}{2}} + aT$). The equations for φ_0 are obtained from equation (2.18) for $\tilde{v}$ and are given in detail in equation (B.2).

For the evolution of ξ_i, it is important that no *new* discontinuities are generated during the computation of transport and source term. This is guaranteed within each timestep Δt using scheme (2.20). To be more precise, the splitting does *not* introduce additional discontinuities due the action of the source term $S(\eta^{(1)}, \eta^{(2)})$ provided that η_0 fulfills (2.24). Note that the same holds for φ provided that $\varphi_i^0 = \mathcal{T}^{-1}\tilde{v}_i^0$ fulfills (2.24).

The evaluation of ξ_j requires us to compute the actual shock positions. Under assumption (2.24), the position of discontinuities in the first component and second component of η at time t^n are given by

$$x_{2i-1}(t^n) = x_{2i-1}(0) + a\,t^n,\ x_{2i}(t^n) = x_{2i}(0) - a\,t^n,\ i = 0,\dots,N_x. \tag{2.25}$$

Here, $x_j(0) = x_{j+\frac{1}{2}}$, and we assume that discontinuities exiting at $x = 1$ (or $x = 0$) enter again at $x = 0$ ($x = 1$).

We turn to the discussion of condition (2.10). In characteristic variables, ℓ_j is the jth unit vector. In the following, we show that the second part of equation (2.10) is always fulfilled. Let i be odd and η be computed by the previous splitting. Then we observe $\Delta_i \eta_x^{(2)} = 0$ since $\eta^{(2)}$ is constant across the position of the discontinuity in the first family $x_{2i-1}(t^n)$. Provided we discretize J such that $\varphi_j^0 := \mathcal{T}^{-1}\tilde{v}_j^0$, $j = 0,\dots,N_x$ in (2.21) also fulfills (2.24), then we have $\Delta_i \varphi^{(2)} = 0$. The same is true for i even and, therefore, the second part of equation (2.10) is fulfilled trivially within the proposed scheme. No additional modification of the scheme is required.

Finally, we consider $J(\eta, y_d) = J(\mathcal{T}y, y_d)$ and obtain the gradient of J in terms of the characteristic variables η and its associated tangent vectors (ϕ, ξ). The detailed equation for $\Delta_{v,\xi} J(\eta, y_d)$ is given in (B.1), with associated discretization given by equation (B.2).

In the following, we describe an algorithm using tangent vectors to solve the optimization problem (2.19). In our description, we may switch between characteristic (η, ϕ) and original variables (y, v) by the linear and time-independent transformation $\mathcal{T}$ defined in equation (2.17). Further, $\tilde{v}$ and v are related by $\tilde{v}(t,x) = v(T-t,x)$ and ϕ and φ are also related by $\varphi(t,x) = \phi(T-t,x)$. We solve problem (2.19) by an iterative scheme starting with an initial guess for the control $u_0 \in U_{ad}$. Herein, U_{ad} is such that $\mathcal{T}^{-1}(u_0, f(u_0)) = \eta_0$ fulfills equation (2.24). Due to the discretization, we have N_x discontinuities in η_0 located at the cell interfaces $x_{i+\frac{1}{2}}$ for all i. With each discontinuity, we have an associated shift ξ_i (independent of time due to equation (2.10)). Further, we have a (discrete) solution y (resp. η) associated with the control η_0. η_0 might not be optimal and should improved. The key to improve the control is equation (2.16) in original variables (see equation (B.1) for a formulation of the relevant term in characteristic variables). In order to fulfill the descent condition (2.16) we *choose* (v, ξ) (resp. (φ, ξ)) such that

$$\Delta_{(v,\xi)} J(y, y_d) \equiv \Delta_{(\varphi,\xi)} J(y, y_d) < 0. \tag{2.26}$$

This choice in original variables is given by equations (2.14) and (2.15). In characteristic variables it is given by equation (B.2) and (B.2c). Note that, in the formulation of $\Delta_{(v,\xi)} J(y, y_d)$, we prescribe terminal data $t = T$ for the L^1-variation v and the the shock shifts ξ. However, our control u_0, resp. η_0, is prescribed at initial time $t = 0$. Therefore, we need to transport the particular choice of $v(T)$ (resp. $\phi(T)$), such that (2.26) holds *backwards* in time using the (discrete) dynamics (2.18) (resp. (2.21)). For simplicity, the backwards-in-time dynamics are transformed into forward-in-time dynamics for the

variables $\tilde{v}$ (resp. φ). In the case of $\xi_i(T)$, the transport backwards in time is trivial, since ξ_i is constant in time. Now, we obtain a new control u_0, resp. η_0 by applying formula (2.13). In the numerical scheme we update the characteristic variable $\eta_0(x)$ by updating the cell average $\eta_{0,i}$ of each component at every spatial point $i=0,\dots,N_x$. We proceed in two steps. First, we add componentwise the cell average of the L^1-part $\varphi_i^{N_t}=\phi_i^0$ in each cell i. Second, we need to take into account the variation $\xi_j(0)$ for each discontinuity j. In characteristic variables, the location of the discontinuity j is computed according to equation (2.25), and it corresponds to the cell index $i(j)$. According to equation (2.23), the solution is piecewise constant on each cell $[x_{i-\frac{1}{2}},x_{i+\frac{1}{2}}]$. Further, it has only discontinuities at every second cell interface in each component. In order to avoid interacting shock shifts, we restrict ρ in equation (2.13) such that $|\xi_i|\le 2\Delta x$. Then, we reconstruct η_0 according to (2.23) and apply the shifts by adding

$$\sum_{i:\xi_i(0)>0}^{N(u_0)} \Delta_i u_0\, \chi_{[x_i(0),x_i(0)+\rho\xi_i(0)]} + \sum_{i:\xi_i(0)<0}^{N(u_0)} \Delta_i u_0\, \chi_{[x_i(0)+\rho\xi_i(0),x_i(0)]}$$

as in equation (2.13). In fact, we add the corresponding term in characteristic variables. We further have to ensure that the new obtained η_0 still fulfills (2.24). Therefore, we need to compute cell averages on $[x_{i-\frac{1}{2}},x_{i+\frac{1}{2}}]$ of the updated control η_0 such that (2.24) holds. Since η_0 was piecewise linear before, the new cell averages are computed exactly.

In the following, we present the update formula in characteristic variables. Denote the volume averaged shifted control in cell j by $\Xi_j^k\,\Delta x$ for the kth component. Then, we obtain

$$\begin{aligned}
\Xi^1_{j-1}=\Xi^1_j=&\min\{(-\bar{\xi}_j)^+,\Delta x\}\eta^{(1),0}_{j+1}+\max\{\bar{\xi}^+_{j-2}-\Delta x,0\}\eta^{(1),0}_{j-1}\\
&+(\Delta x-\min\{(-\bar{\xi}_j)^+,\Delta x\}-\max\{\bar{\xi}^+_{j-2}-\Delta x,0\})\eta^{(1),0}_j, &\text{(2.27a)}\\
\Xi^2_{k-1}=\Xi^2_k=&\min\{(-\bar{\xi}_k)^+,\Delta x\}\eta^{(2),0}_{k+1}+\max\{\bar{\xi}^+_{k-2}-\Delta x,0\}\eta^{(2),0}_{k-1}\\
&+(\Delta x-\min\{(-\bar{\xi}_k)^+,\Delta x\}-\max\{\bar{\xi}^+_{k-2}-\Delta x,0\})\eta^{(2),0}_k, &\text{(2.27b)}\\
\tilde{\eta}^{(1),0}_i=&\frac{\Xi^1_i}{\Delta x}-\varphi^{(1),N_t}_i, &\text{(2.27c)}\\
\tilde{\eta}^{(2),0}_i=&\frac{\Xi^2_i}{\Delta x}-\varphi^{(2),N_t}_i. &\text{(2.27d)}
\end{aligned}$$

Herein, the current cell average of the control is denoted by η_i^0, and the update is denoted by $\tilde{\eta}_i^0$. The index $j\in\{0,\dots,N_x\}$ is odd, and $k\in\{0,\dots,N_x\}$ is even. Further, we denote by $x^+=\max\{x,0\}$ and by $\bar{\xi}_i=\mathcal{P}(-\xi_i)$ where $\mathcal{P}$ is the projection on $[-2\Delta x,2\Delta x]$, i.e.,

$$\mathcal{P}(z)=\begin{pmatrix} -2\Delta x & z\le -2\Delta x\\ z & -2\Delta x<z<2\Delta x\\ 2\Delta x & z\ge 2\Delta x\end{pmatrix}.$$

Those computations are exemplified in Remark 2.2. Summarizing, in (2.27), a piecewise constant reconstruction of $\tilde{\eta}$ is computed where, for example, in the case of the first component the discontinuity at $x_{i+\frac{1}{2}}$ is moved by ξ_i and at $x_{i-\frac{3}{2}}$ by ξ_{i-2}. Since φ fulfills (2.24), this holds for $\tilde{\eta}$.

The previous computation leads to an iterative algorithm for numerically solving (2.19) or equivalently

$$\min_{\eta_0\in\mathcal{U}} J(\mathcal{T}\eta,y_d) \text{ sbj to } y=\mathcal{T}\eta,(2.2),\eta(0,x)=\eta_0(x),\eta(t,0)=\eta(t,1) \text{ and } (2.24).$$

Algorithm

1. Set terminal time $T>0$ and $a^2 \geq \max_{y^{(1)}}(f'(y^{(1)})^2$, and choose an equidistant spatial discretization with N_x gridpoints. Choose $\Delta t = \frac{\Delta x}{a}$ and $\mathbf{k}=0$. Let $\eta_{0,i}^{\mathbf{k}} = \left((\eta_{0,i}^{(1)})^{\mathbf{k}}, (\eta_{0,i}^{(2)})^{\mathbf{k}}\right)$ for $i=0,\dots,N_x$ be an arbitrary initial control such that $\eta_0^{\mathbf{k}}$ fulfills (2.24). Let $(y_d)_i$ be a discretization of the given function $y_d(\cdot)$.
2. Solve equation (2.20) with initial data $(y_0)_i := \mathcal{T}\eta_{0,i}^{\mathbf{k}}$ to obtain $\eta_i^{N_t} = \mathcal{T}^{-1} y_i^{N_t}$.
3. Set initial data φ_i^0 and shock variations ξ_i given by equation (B.2). Therein, $x_i(t^{N_t})$ are given by equation (2.25).
4. Solve equation (2.21) for initial data $\tilde{v}_i^0 := \mathcal{T}\varphi_i^0$ to obtain $\varphi_i^{N_t} = \mathcal{T}^{-1}\tilde{v}_i^{N_t}$.
5. Obtain the new iterate $\eta_{0,i}^{\mathbf{k+1}} := \tilde{\eta}_i^0$ where $\tilde{\eta}_i^0$ is given by equation (2.27). To evaluate equation (2.27) use the old iterate as $\eta_i^0 := \eta_{0,i}^{\mathbf{k}}$, the solution $\varphi_i^{N_t}$ and the shifts ξ_i.
6. Provided that $J(\mathcal{T}\eta, y_d)$ is sufficiently small, we terminate. Otherwise, set $\mathbf{k} \to \mathbf{k}+1$ and continue with Step 2.

REMARK 2.2. Note that $\eta_{0,i}^{\mathbf{k}}$ is a vector of two components. The algorithm computes a sequence $\left((\eta_{0,i}^{\mathbf{k}})_{i=0}^{N_x}\right)_{\mathbf{k}=0}^{\infty}$ of approximations

$$y^{\mathbf{k}}(0,x) = \sum_{i=0}^{N_x} \chi_{\left[x_{i-\frac{1}{2}}, x_{i+\frac{1}{2}}\right]} \mathcal{T}\eta_{0,i}^{\mathbf{k}}$$

to the optimal control $y^*(0,x)$ of problem (2.19). During the iteration on $\mathbf{k}$, the data φ_i^0 and ξ_i are chosen in every step such that the gradient of the objective function is non-positive, see equation (B.1) and equation (B.2). The derivative of the objective functional is computed at terminal time T using the solution η at time T. The update for the control $\eta_{0,i}$ has to be at initial time. Therefore, in Step 4, the algorithm propagates the information backwards using equation (2.21). At initial time, the variations in L^1 and for the shock position are added towards the old control $\eta_{0,i}^{\mathbf{k}}$ in order to obtain an improved control for the next iteration $\mathbf{k+1}$. Using this new control, equation (2.20) will be solved. If the mismatch in the objective functional is still large enough, the procedure is repeated.

We present more details on the motivation of equation (2.27) where the values Ξ_j are introduced. Those values describe the effect of the shift in the discontinuity on the values of η_i^0 and are used in Step 5 of the algorithm. We consider the first component only with the other being similar. Due to the construction of the discretized control $\eta_i^{(1),0}$ we have a discontinuity only at indices i when i is odd. More precisely, located at position $x_{i+\frac{1}{2}}$ for i odd. From Step 4, we obtain the shift ξ_i in the shock position. We revert the sign of ξ_i in order to obtain a descent in the objective function (see equation for $\bar{\xi}_i$ below). Since we require equation (2.24) to hold, we first project the shift ξ_i onto the interval $[-2\Delta x, 2\Delta x]$ and denote the projection by $\bar{\xi}_i = \mathcal{P}(-\xi_i)$. Assume now $-\Delta x < \bar{\xi}_i < 0$. Then, in order to have a piecewise constant control on the spatial intervals $[x_{i-\frac{1}{2}}, x_{i+\frac{1}{2}}]$ we need to shift the current control at point $x_{i+\frac{1}{2}}$ by ξ_i and average again the shifted control on $[x_{i-\frac{1}{2}}, x_{i+\frac{1}{2}}]$. This way, we obtain $\eta_{0,i}^{(1)}$. Assume no other shift has happened. Then, the volume average of the shifted control in cell i is given by

$$\eta_{0,i}^{(1)} = \frac{1}{\Delta x}\left((-\bar{\xi}_i)\eta_{0,i+1}^{(1)} + (\Delta x - (-\bar{\xi})\eta_{0.i}^{(1)})\right) = \frac{\Xi_i^1}{\Delta x}.$$

The formula, equation (2.27), is obtained when taking into account shifts in positive and negative direction as well as shifts of the neighboring cells.

Note that, in the case $\xi_i \equiv 0$ for all i, we obtain $\frac{\Xi_i^1}{\Delta x} = \eta_i^{(1),0}$.

Compared to the general case given by equation (2.13), we presented the algorithm for $\rho \equiv 1$. In the numerical results, we observed convergence even in this case. However, it is only a minor modification to include $0 < \rho < 1$ in Step 5. Note that including a $\rho > 0$ requires us also to introduce a stepsize control mechanism such as, for example, Armijo's rule.

3. Numerical results

We present numerical results using the previous calculus for two cases. The simplest possible application is the optimal control of a linear system (2.2) *without* source term. Second, we present results on the optimal control for the relaxation system (2.2) for Burgers' flux $f(w) = \frac{1}{2}w^2$. All spatial grids are equidistant on $I = [0,1]$ and the temporal discretization is such that the CFL condition [15] is satisfied. We use periodic boundary conditions in all cases. The cost functional J is discretized using the trapezoidal rule. All initial controls are constant with $\eta_0(x) = (\frac{1}{2}, \frac{1}{4})$. Numerical tests not reported here show first-order convergence of the scheme. We observe that the applied modifications to the IMEX scheme do not alter the properties of the original scheme proposed in [25].

The minimization problem (1.1) does not necessarily have a unique solution. This is, for example, the case if the desired state is generated by a strong discontinuity. Therefore, the initial value for the optimization might have a strong influence on the local minimizer found. The non-uniqueness of the minimization problem has been discussed in recent literature as for example [1]. Our purpose of studying problem (1.1) is to exemplify the numerical application of the tangent vector calculus. Therefore, we do not focus on possible non-uniqueness of the solution to (1.1).

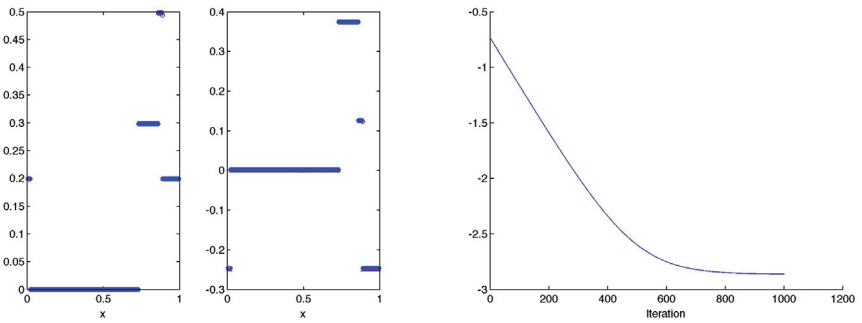

FIG. 3.1. *Desired state (red crosses) and optimized state (blue circles) for the linear system with* $N_x = 200$ *grid points in space for both components* $(y^{(1)}, y^{(2)})$ *in the left part of the figure. The pointwise difference of optimized and desired state is given in Figure 3.2. Iteration history in* log*-scale for the cost. The spatial resolution of the scheme is* $\Delta x = 5 \times 10^{-3}$ *and* $\log_{10}(\Delta x) \approx -2.3$.

3.1. Optimal control of a linear system. We consider problem (3.1) with periodic boundary conditions on the domain $x \in I$, $T = 0.35$ and $a^2 = \frac{5}{4}$.

$$\min_{u_0} \int_0^1 \left(y^{(1)}(T,x) - y_d^{(1)}(x) \right) dx \text{ sbj to } y_t + \begin{pmatrix} 0 & 1 \\ a^2 & 0 \end{pmatrix} y_x = 0,\ y(0,x) = (u_0(x), f(u_0)). \tag{3.1}$$

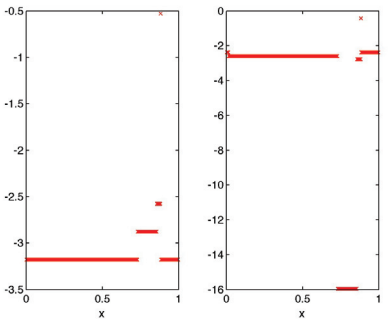

FIG. 3.2. *Pointwise difference of desired state and optimized state in logarithmic scale for the linear system with $N_x = 200$ grid points in space for both components $(y^{(1)}, y^{(2)})$. The corresponding profiles are depicted in Figure 3.1.*

In the example, we initialize the control similar to (2.3) and $f(w) = \frac{1}{2}w^2$. The desired state y_d is depicted in Figure 3.1 (along with the obtained optimized state). The pointwise errors in terminal state are depicted in Figure 3.2. The corresponding initial data $y(0,x) = (u_0(x), f(u_0))$ corresponding to the desired state y_d is given by

$$u_0(x) = \begin{pmatrix} 1 & 0.30 \le x \le 0.45 \\ 0.1 & 0.5 \le x \le 0.65 \\ 0 & \text{else} \end{pmatrix}.$$

The algorithm is started with constant control η_0 and stopped after at most 2000 steps of iteration. The iteration history is depicted in the right part of Figure 3.1. With the proposed method we observe convergence until the grid resolution is reached. The dependence on the spatial grid is given in Table 3.1. As expected we observe first-order convergence.

N_x	J	Rate	$\|y_0^{(1)} - y_*^{(1)}(t=0,\cdot)\|_2$	Rate	$\|y_0^{(2)} - y_*^{(2)}(t=0,\cdot)\|_2$	Rate
50	$4.6936e-03$	(0.00)	$5.5364e-03$	(0.00)	$6.9206e-03$	(0.00)
100	$2.5878e-03$	(0.91)	$2.8922e-03$	(0.96)	$3.6152e-03$	(0.96)
200	$1.3510e-03$	(0.96)	$1.4739e-03$	(0.98)	$1.8424e-03$	(0.98)
400	$9.9964e-04$	(0.68)	$8.2176e-04$	(0.90)	$1.2031e-03$	(0.77)

N_x	$\|y_d^{(1)} - y_*^{(1)}(t=T,\cdot)\|_2$	Rate	$\|y_d^{(2)} - y_*^{(2)}(t=T,\cdot)\|_2$	Rate
50	$5.5364e-03$	(0.00)	$6.9206e-03$	(0.00)
100	$2.8922e-03$	(0.96)	$3.6152e-03$	(0.96)
200	$1.4739e-03$	(0.98)	$1.8424e-03$	(0.98)
400	$7.5945e-04$	(0.97)	$1.2666e-03$	(0.73)

TABLE 3.1. *Convergence history for different spatial grids with N_x equidistant grid points. Reported are the value of the cost functional J after optimization, the L^2-norm difference of both components $(y^{(1)}, y^{(2)})$ for the initial data $y_0 = y(0,x)$, and the desired state y_d. The optimized solution is denoted by $y_*(t,x)$.*

We compare the obtained results also to the case when the shock variations ξ_i are *not* taken into account. Hence, we consider the same example as before and run the same algorithm *but* set $\xi_i \equiv 0$ for $j = 1,2$ in equation (2.27). The dependence on the spatial grid in this situation is depicted in Table 3.2. Comparing to Table 3.1, we observe a deterioration in the convergence rate from ≈ 1 when including the shock variations to $\approx \frac{1}{2}$ for the cost functional and $\approx \frac{3}{4}$ for state when neglecting this contribution.

Note that the error in the second component is smaller compared to the scheme neglecting the shock sensitivities. In the first component and the functional, we observe the opposite behavior. However, the overall resolution is always below the numerical resolution of the grid, and, therefore, a comparison of those values is difficult.

N_x	J	Rate	$\|y_0^{(1)} - y_*^{(1)}(t=0,\cdot)\|_2$	Rate	$\|y_0^{(2)} - y_*^{(2)}(t=0,\cdot)\|_2$	Rate
50	$9.8550e-04$	(0.00)	$1.9823e-03$	(0.00)	$3.6662e-03$	(0.00)
100	$9.8310e-04$	(0.50)	$1.3402e-03$	(0.74)	$2.6691e-03$	(0.69)
200	$9.9839e-04$	(0.49)	$9.5812e-04$	(0.70)	$1.8837e-03$	(0.71)
400	$9.9986e-04$	(0.50)	$6.7520e-04$	(0.71)	$1.3360e-03$	(0.70)

N_x	$\|y_d^{(1)} - y_*^{(1)}(t=T,\cdot)\|_2$	Rate	$\|y_d^{(2)} - y_*^{(2)}(t=T,\cdot)\|_2$	Rate
50	$1.6294e-03$	(0.00)	$3.9955e-03$	(0.00)
100	$1.0328e-03$	(0.79)	$2.8747e-03$	(0.69)
200	$7.3280e-04$	(0.70)	$2.0440e-03$	(0.70)
400	$4.9368e-04$	(0.74)	$1.4578e-03$	(0.70)

TABLE 3.2. *Convergence history for different spatial grids with N_x equidistant grid points* neglecting *the effect of the shock variations ξ_i on the optimal control. As in Table 3.1, we report the value of the cost functional J after optimization, the L^2-norm difference of both components $(y^{(1)}, y^{(2)})$ for the initial data $y_0 = y(0,x)$, and the desired state y_d. The optimized solution is denoted by $y_*(t,x)$.*

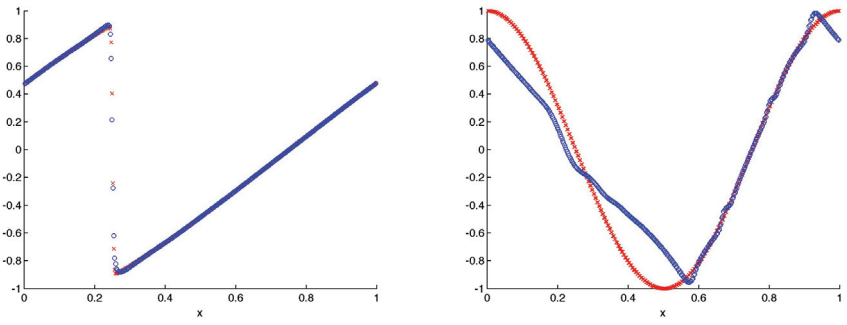

FIG. 3.3. *Desired state (red crosses) and optimized state (blue circles) for the linear system with $N_x = 400$ grid points in space for the variable $y^{(1)}(T,x)$ in the left part of the figure and for $y^{(1)}(0,x)$ in the right part.*

3.2. Optimal control of the relaxation approximation to Burgers' equation. We consider problem (3.1) with $T = 0.35$, $\epsilon = 10^{-4}$, $N_x = 400$, and $a = \frac{5}{4}$. The desired state y_d is the solution at time T to (2.2) and (2.3) for $u_0(x) = \cos(2\pi x)$. The algorithm is started with constant control η_0 and stopped after the value of the cost functional is below 10^{-4}. We depict desired and optimized state in the original variables $y(T,\cdot)$ in Figure 3.3. The obtained optimized control $\eta_0^{\mathbf{k}}$ and the function u_0 are depicted in Figure 3.3 and the iteration history in Figure 3.4.

We observe a good agreement in the recovered desired state y_d. The difference in the obtained control is due to the fact that the solution to equation (2.19) is not unique.

In Figure 3.5 and Figure 3.6, we present a similar example but with desired state y_d obtained as solution to (2.2) and (2.3) for $u_0(x) = \chi_{[0.3,0.45]}(x)$. All other parameters are as before. Similar to the previous results, we observe that there is no uniqueness in the control u_0 leading to y_d.

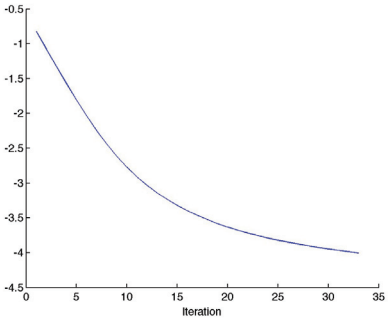

FIG. 3.4. *Iteration history for the example of Figure 3.3 in* log*-scale for the value of the cost functional* J*. The stopping criteria is* $J \leq 10^{-4}$*, which is comparable with the spatial resolution of the scheme,* $\Delta x = 2.5 \times 10^{-3}$.

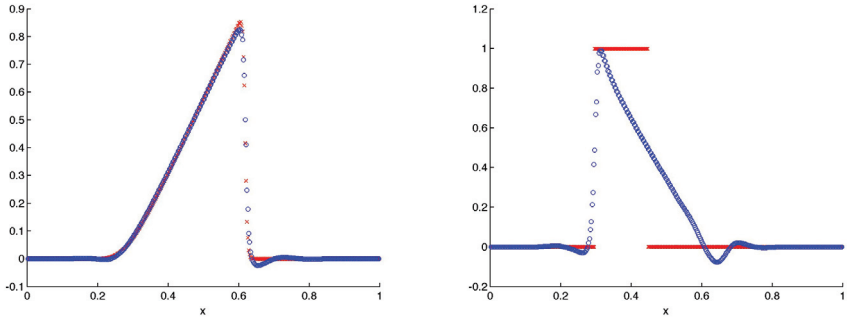

FIG. 3.5. *Desired state (red crosses) and optimized state (blue circles) for the linear system with* $N_x = 400$ *grid points in space for the variable* $y^{(1)}(T,x)$ *in the left part of the figure and for* $y^{(1)}(0,x)$ *in the right part.*

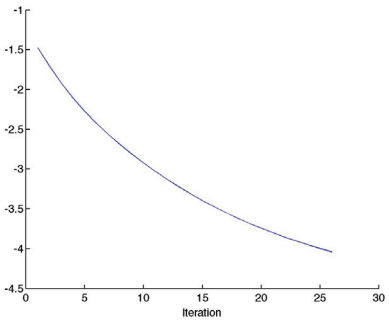

FIG. 3.6. *Iteration history for the example of Figure 3.3 in* log*-scale for the value of the cost functional* J*. The stopping criteria is* $J \leq 10^{-4}$*, which is comparable with the spatial resolution of the scheme,* $\Delta x = 2.5 \times 10^{-3}$.

4. Summary

We present a numerical method for solving optimal control problems subject to the relaxation approximation to hyperbolic conservation laws. Equations for the evolution of the corresponding tangent vector of the relaxation system have been derived, and

a numerical discretization has been introduced. The tangent vector has been used to compute the analytical gradient of the reduced cost also in the presence of traveling discontinuities. A numerical discretization of the gradient has been implemented to solve some examples of linear and nonlinear optimal control problems. The computation of the finite dimensional part of the tangent vector allows us to obtain the expected order of convergence.

We comment on Table 3.1 and Table 3.2. Compared to the method ignoring the shifts in the tangent vectors, we observed an improved numerical performance. However, the improvement yields only higher convergence rates, not necessarily smaller residuals (up to the chosen tolerance). This is not contradictory to the theoretical result. Therein, we only to expect residuals as low as the numerical discretization error. The iterative procedure using shifts does not yield the same iterates and includes a projection towards the piecewise constant control. This introduces an error of the order of the grid, which may explain the higher residuals. In the linear example where the exact solution is known, this solution can be obtained either using the shifts or using suitable updates of the cell averages and ignoring the shifts. This is due to the linear structure of the problem. But neglecting shifts yields a different approximation to the optimization problem. In particular, this is *not* the theoretically correct one. Nevertheless, it yields smaller numerical residuals. A possible reason might be that, when ignoring the shifts, we update on N_x cells cell averages. The true solution, however, requires only two correct shock positions. Therefore, there are more degrees of freedom, possibly leading to smaller residuals.

Appendix A. Definitions and supplementary lemmas.

In this section, we collect definition and statements from the [8,10]. They are given for the sake of completeness.

DEFINITION A.1 (Continuous path). *A mapping $\gamma:[a,b]\to L^1(\mathbb{R}^n)$ is called a continuous path if γ is continuous on the interval $[a,b]$ with respect to L^1-norm, i.e.,*

$$\forall x\in[a,b]:\lim_{\epsilon\to 0}\|\gamma(x+\epsilon)-\gamma(x)\|_{L^1}=0.$$

DEFINITION A.2 (Broad solution). *Consider the quasi-linear partial differential equation*

$$u_t(t,x)+A(t,x)u_x(t,x)=h(t,x,u), \tag{A.1}$$

where $A\in\mathbb{R}^{n\times n}$ is strictly hyperbolic, Lipschitz and h is measurable w.r.t. (t,x) and Lipschitz continuous w.r.t. u. Assume an initial condition $u(0,x)=u^0(x)$ with $u_0\in L^1(\mathbb{R};\mathbb{R}^n)$. Denote by ℓ_i,r_i the ith left and right eigenvectors of A. Denote by λ_i the ith eigenvalues of A. We denote by $t\to y_i(t;\tau,\xi)$ the solution to the Cauchy problem

$$\frac{d}{dt}y(t)=\lambda_i(t,y(t)),\ y(\tau)=\xi.$$

Denote by $<,>$ the scalar product on $\mathbb{R}^n$ and by

$$g_i:=<\ell_i,h>+<\partial_t\ell_i+\lambda_i\partial_x\ell_i,u>,\ u=\sum u_ir_i.$$

We define a broad solution $u=\sum u_ir_i$ to equation (A.1) *as a locally integrable function fulfilling*

$$\frac{d}{dt}u_i(t,y_i(t;\tau,\xi))=g_i(t,y_i(t;\tau,\xi),u(t,y_i(t;\tau,\xi))$$

in the sense that, for a.e. (τ,ξ) *and all* $i=1,\dots,n$*, the following holds:*

$$u_i(\tau,\xi)=u_i^0(y_i(0;\tau,\xi))+\int_0^\tau g_i\,(s,y_i(s;\tau,\xi),u(s,y_i(s;\tau,\xi))\,ds.$$

The main result used in this work is [8, Theorem 2.2]. We recall the statement for convenience.

Consider the equation

$$\partial_t u+\partial_x F(u)=h(t,x,u) \tag{A.2}$$

supplemented with initial data $u(0,x)=u_0(x)$ and the following assumptions:

(H1) The vector field $F:\Omega\to\mathbb{R}^n$ is $\mathcal{C}^2$, where $\Omega\subset\mathbb{R}^n$ is closed and bounded. For each $u\in\Omega$, the matrix $A(u)=DF(u)$ has n real distinct eigenvalues. Its eigenvalues λ_i and its left and right eigenvectors ℓ_i and r_i, respectively, are normalized such that $<\ell_i,r_j>=\delta_{ij}$. Denote by

$$A(u,v)=\int_0^1 A(\theta u+(1-\theta)v)d\theta$$

with corresponding eigenvectors $\ell_i(u,v)$, $r_i(u,v)$ and eigenvalues $\lambda_i(u,v)$. Suppose that $\ell_i(u,v)$,$r_i(u,v)$ and $\lambda_i(u,v)$ are uniformly bounded for all $u,v\in\Omega$.

(H2) Denote by $\hat{\lambda}$ the uniform bound on $\lambda_i(i,v)$ for all i. Then, solutions to (A.2) are considered in the domain

$$\mathcal{D}:=\{(t,x):0\le t\le T,x\in[a+\hat{\lambda}t,b-\hat{\lambda}t]\}.$$

Assume further that the function $h:\mathcal{D}\times\Omega\to\mathbb{R}^n$ is bounded and continuously differentiable.

(H3) Whenever $u^+\in\Omega$ and $u^-\in\Omega$ are connected by a shock or a contact discontinuity, say of the kth characteristic family, the linear system

$$0=\Phi_i(u^+,u^-,w^+,w^-)=\sum_{j=1}^n <D\ell_i(u^+,u^-)\cdot(w_j^+r_j^+,w_j^-r_j^-),u^+-u^->$$
$$+\sum_{j=1}^n <\ell_i(u^+,u^-),w_j^+r_j^+-w_j^-r_j^->,\forall i\neq k$$

can be uniquely solved in terms of the outgoing variables $w_{j^\pm}^\pm$ $j^\pm\in\{j^-:j<k\}\cup\{j^+:j>k\}=:\mathcal{O}$. Assume that the function W_j defined by

$$w_j^\pm=W_{j^\pm}(u^+,u^-)((w_j)_{j^\pm\notin\mathcal{O}}),\ j\neq k,j^\pm\in\mathcal{O}$$

satisfies a bound of the form

$$\|W_{j^\pm}(u^+,u^-)((w_j)_{j^\pm\notin\mathcal{O}})\|\le C\|(w_j)_{j^\pm\notin\mathcal{O}}\|.$$

Here, $r_j^\pm=r_j(u^\pm)$. For a definition of the class of functions which are piecewise Lipschitz with simple discontinuities, we refer to [8].

THEOREM A.3. *Let the assumptions* $(H1)-(H3)$ *hold. Let* u *be a piecewise Lipschitz continuous solution to equation* (A.2) *with* u^0 *in the class PLSD. Let* $(v_0,\xi_0)\in L^1\times\mathbb{R}^N$ *be a tangent vector to* u^0 *generated by a regular variation* $\gamma:\delta\to u^0_\delta$*, Let* u_δ *be the solution of equation* (A.2) *with initial condition* u^0_δ*. Then, there exists* $\tau_0>0$ *such that, for all* $t\in[0,\tau_0]$*, the path* $\bar\gamma:\delta\to u_\delta$ *is a regular variation for* $u_\delta(t,\cdot)$ *generating the tangent vector* $(v(t),\xi(t))\in L^1\times\mathbb{R}^N$*. The vector is the unique broad solution of the initial boundary value problem*

$$\begin{aligned}\xi(0)=\xi_0, v(0,x)=v_0(x),\\ v_t+A(u)v_x+(DA(u)v)u_x=h_u(t,x,u)\end{aligned}$$

outside the discontinuities of u*, while for* $\alpha=1,\dots,N$*,*

$$\begin{aligned}<D\ell_i(u^+,u^-)\cdot(v^++\xi_\alpha u_x^+,v^-+\xi_\alpha u_x^-),u^+-u^->=\\ +<\ell_i(u^+,u^-),v^++\xi_\alpha u_x^+-v^--\xi_\alpha u_x^->, i\neq k_\alpha,\\ \frac{d}{dt}\xi_\alpha=D\lambda_{k_\alpha}(u^+,u^-)(v^++\xi_\alpha u_x^+,v^-+\xi_\alpha u_x^-)\end{aligned}$$

along each line $x=x_\alpha(t)$*, where* u *suffers a discontinuity in the* k_α *characteristic direction.*

The technical details are given in [8]. We motivate the result by the following explanation. The equation for v is independent of the equation for ξ_α and can therefore be solved separately. The equation is formally derived by differentiation of the conservation law (A.2) with respect to u in direction v. It describes the sensitivity of the L^1-part of the solution. The equation is linear in v but not in conservative form and with possibly discontinuous coefficient due to discontinuities in u. Along those discontinuities, the equations for ξ_α and the algebraic condition needs to hold.

Assume u is discontinuous across $(t,x_\alpha(t))$. Then, for u to be a weak solution, the Rankine–Hugoniot condition needs to be fulfilled. The condition is $s[u]=[F(u)]$. Denoting the left- and right-sided limits $u(t,x_\alpha(t)\pm)$ by $u\pm$, respectively, the previous equation may be rewritten as

$$\lambda(u^+,u^-)(u^+-u^-)=A(u^+,u^-)(u^+-u^-)$$

using the average matrix $A(u^+,u^-)$ introduced in (H1) and using that the shock speed s is equal to an eigenvalue $\lambda(u^+,u^-)$ of the matrix $A(u^+,u^-)$. If x_α is a discontinuity in the k_α family, then the previous equation can be reduced to

$$\frac{d}{dt}x_\alpha(t)=\lambda_{k_\alpha}(u^+,u^-),<\ell_i(u^+,u^-),u^+-u^->=0\,\forall i\neq k_\alpha.$$

According to the notion of derivatives, we need to consider a variation not only in the L^1 part but also in the shock position. Formally, this corresponds to considering the $O(\epsilon)$ perturbation of $u^\pm=u(t,x_\alpha(t))$ as

$$u^\pm_\epsilon=u(t,x_\alpha(t)\pm\epsilon\xi_\alpha(t))+\epsilon v(t,x_\alpha(t)).$$

Assuming the perturbation $x_\alpha(t)+\epsilon\xi_\alpha(t)$ also fulfills the previous set of equations, we may compute the formal limit for $\epsilon\to0$. Hence, we obtain up to $O(\epsilon^2)$

$$\frac{d}{dt}\xi_\alpha(t)=D\lambda_{k_\alpha}(u^+,u^-)(u_x^+\xi_\alpha+v^+,u_x^-\xi_\alpha+v^-)$$

and similar for the second algebraic equation. The second algebraic condition is interpreted as follows: a shift variation in the k_α family leads to a modified function which only suffers discontinuities in the *same* k_α family but *not* in any other family $i \neq k_\alpha$.

Appendix B. The expression of objective and tangent vectors in characteristic variables. The gradient of the objective functional J in terms of characteristic variables η and the associated tangent vector (ϕ,ξ) is given by

$$\begin{aligned}\Delta_{(\phi,\xi)}J(\eta,y_d) = &\frac{1}{2}\int \chi_I(x)\left(\frac{\eta^{(1)}(T,x)-\eta^{(2)}(T,x)}{2a}-y_d(x)\right)\phi^{(1)}(T,x)dx\\ &-\frac{1}{2}\int \chi_I(x)\left(\frac{\eta^{(1)}(T,x)-\eta^{(2)}(T,x)}{2a}-y_d(x)\right)\phi^{(2)}(T,x)dx\\ &+\frac{1}{2}\sum_{j=1}^{N(u_0)}\left\{\left(\frac{\eta^{(1)}(T,x_j(T)+)-\eta^{(2)}(T,x_j(T)+)}{2a}-y_d(x_j(T)+)\right)\right.\\ &\left.+\left(\frac{\eta^{(1)}(T,x_j(T)-)-\eta^{(2)}(T,x_j(T)-)}{2a}-y_d(x_j(T)-)\right)\right\}\times\xi_j(T)\\ &\times\left(\Delta_j\eta^{(1)}(T,\cdot)-\Delta_j\eta^{(2)}(T,\cdot)\right),\end{aligned} \tag{B.1}$$

where $\Delta_j w(\cdot) = w(x_j(T)+) - w(x_j(T)-)$. Note that, in the last terms, the evaluation of η at time T is at point $x_j(T)$. This point is the terminal point of the jth discontinuity in the initial data η_0 propagated forward to terminal time T. The value of x_j is computed by moving the jth discontinuity with speed $\pm a$ depending on whether it is a jump in the first or second component, see equation (2.25). For example, in equation (B.1), we have $x_j = x_j(0) - aT$ for all even indices j.

Since $\varphi(t,x) = \phi(T-t,x)$ we have $\varphi(0,x) = \phi(T,x)$. Then, similarly to (2.13), we may use (B.1) to determine a descent direction for J by the following discretization for $i = 0,\dots,N_x$ and with φ_i^0 as discretization of $\varphi(0,x_i)$.

$$\varphi_{2i}^{(1),0} = \phi_{2i}^{(1),N_t} = \frac{\eta_{2i}^{(1),N_t} - \eta_{2i}^{(2),N_t}}{2a} - (y_d)_{2i},\ \varphi_{2i+1}^{(1),0} = \varphi_{2i}^{(1),0}, \tag{B.2a}$$

$$\varphi_{2i-1}^{(2),0} = \phi_{2i-1}^{(2),N_t} = -\left(\frac{\eta_{2i-1}^{(1),N_t} - \eta_{2i-1}^{(2),N_t}}{2a} - (y_d)_{2i-1}\right),\ \varphi_{2i}^{(2),0} = \varphi_{2i-1}^{(2),0}. \tag{B.2b}$$

In the present case, we have $N(u_0) = N(\eta_0) = N_x$ since at each cell interface there is a discontinuity in the initial data η_0. Recall that we have discontinuities in the first family only at odd indices and in the second family at even indices. We prescribe $\xi_j(T)$ for the jth discontinuity at terminal time and propagate backwards in time by equation (2.10) (i.e., $\xi_j(T) = \xi_j(0)$ for all discontinuities $j = 0,\dots,N_x$). Denote by $\Delta_j w(\cdot) = w(x_{j+1}) - w(x_j)$ and by $\overline{\Delta}_j w(\cdot) = \frac{1}{2}(w(x_{j+1}) + w(x_j))$. Due to the choice of $\Delta t = \frac{\Delta x}{a}$ and $T = N_t\,\Delta t$, we have that a shock j located initially at the cell interface $x_j(0) = x_{j+\frac{1}{2}}$ and moving at speed a is located at time T at $x_j(T)$ being again a cell interface located at $x_{i+\frac{1}{2}} = x_{j+\frac{1}{2}} + aT$ for some $i \in \{0,\dots,N_x\}$. We denote by $i(j)$ this location. Note that, for j odd (even), the speed of the discontinuity is $-a$ (a), as in equation (2.25). The jth discontinuity is by convention located initially at $x_j(0) = x_{j+\frac{1}{2}}$.

$$\xi_j = \xi_j(T) = \frac{1}{2}\left(\left(\overline{\Delta}_{i(j)}\eta^{(1),N_t} - \overline{\Delta}_{i(j)}\eta^{(2),N_t} - \overline{\Delta}_{i(j)}y_d\right)\times\left(\widehat{\Delta}_{i(j)}\eta^{(1),N_t} - \widehat{\Delta}_{i(j)}\eta^{(2),N_t}\right)\right). \tag{B.2c}$$

where $\overline{\Delta} w_k = \frac{1}{2a}(w_{k+1} + w_k)$ and $\widehat{\Delta} w_k = w_{k+1} - w_k$. Note that the formula simplifies if this term is evaluated in original variables y instead of η. However, in order to show the relation to equation (B.1), we write here the technical formulation.

Acknowledgments. This work has been supported by DFG Cluster of Excellence EXC128, RWTH Seedfund project, the BMBF KinOpt Project and NSF KI-Net.

REFERENCES

[1] M.K. Banda and M. Herty, *Adjoint IMEX-based schemes for control problems governed by hyperbolic conservation laws*, Comput. Optim. Appl., 51(2), 909–930, 2012.

[2] C. Bardos and O. Pironneau, *A formalism for the differentiation of conservation laws*, C.R. Math. Acad. Sci. Paris, 335(10), 839–845, 2002.

[3] S. Bianchini, *On the shift differentiability of the flow generated by a hyperbolic system of conservation laws*, Discrete Contin. Dynam. Systems, 6, 329–350, 2000.

[4] S. Bianchini, *Hyperbolic limit of the Jin-Xin relaxation model*, Commun. Pure Appl. Math., 59(5), 688–753, 2006.

[5] F. Bouchut and F. James, *One-dimensional transport equations with discontinuous coefficients*, Nonlinear Anal., 32(7), 891–933, 1998.

[6] F. Bouchut and F. James, *Differentiability with respect to initial data for a scalar conservation law*, in hyperbolic problems: Theory, Numerics, Applications, Vol. I (Zürich, 1998), Internat. Ser. Numer. Math., Birkhäuser, Basel, 113–118, 129, 1999.

[7] A. Bressan and G. Guerra, *Shift-differentiability of the flow generated by a conservation law*, Discrete Contin. Dynam. Systems, 3, 35–58, 1997.

[8] A. Bressan and A. Marson, *A maximum principle for optimally controlled systems of conservation laws*, Rend. Sem. Mat. Univ. Padova, 94, 79–94, 1995.

[9] A. Bressan and W. Shen, *Optimality conditions for solutions to hyperbolic balance laws*, Contemporary Mathematics, 426, 129, 2007.

[10] A. Bressan, *Hyperbolic systems of conservation laws*, in Oxford Lecture Series in Mathematics and its Applications, Oxford University Press, Oxford, 20, 2000.

[11] A. Bressan, G. Crasta, and B. Piccoli, *Well-posedness of the Cauchy problem for $n \times n$ systems of conservation laws*, Mem. Amer. Math. Soc., 146(694), viii+134, 2000.

[12] A. Bressan and A. Marson, *A variational calculus for discontinuous solutions of systems of conservation laws*, Commun. Part. Diff. Eqs., 20(9-10), 1491–1552, 1995.

[13] C. Castro, F. Palacios, and E. Zuazua, *An alternating descent method for the optimal control of the inviscid Burgers equation in the presence of shocks*, Math. Models Meth. Appl. Sci., 18, 369–416, 2008.

[14] A. Chertock, M. Herty, and A. Kurganov, *An Eulerian–Lagrangian method for optimization problems governed by multidimensional nonlinear hyperbolic PDEs*, Computational Optimization and Applications, 1–36, 2014.

[15] R. Courant, K.O. Friedrichs, and H. Lewy, *Über die partiellen Differenzengleichungen der Mathematischen Physik*, Mathematische Annalen, 100(1), 32–74, 1928.

[16] C. D'Apice, R. Manzo, and B. Piccoli, *Numerical schemes for the optimal input flow of a supply chain*, SIAM J. Numer. Anal., 51(5), 2634–2650, 2013.

[17] C. D'Apice, S. Göttlich, M. Herty, and B. Piccoli, *Modeling, Simulation, and Optimization of Supply Chains: A Continuous Approach*, SIAM, Philadelphia, PA, 2010.

[18] M. Giles and E. Sueli, *Adjoint methods for PDEs: a posteriori error analysis and postprocessing by duality*, Acta Numerica, 11, 145–236, 2002.

[19] M. Giles and S. Ulbrich, *Convergence of linearized and adjoint approximations for discontinuous solutions of conservation laws: Part 1: Linearized approximations and linearized output functional*, SIAM J. Numer. Anal., 48, 882–904, 2010.

[20] M. Giles, *Analysis of the accuracy of shock-capturing in the steady quasi 1d-euler equations*, Int. J. Comput. Fluid Dynam., 5, 247–258, 1996.

[21] E. Godlewski and P.A. Raviart, *The linearized stability of solutions of nonlinear hyperbolic systems of conservation laws. A general numerical approach*, Math. Comput. Simulation, 50(1-4), 77–95, 1999. Modelling '98 (Prague).

[22] M. Gugat, M. Herty, A. Klar, and G. Leugering, *Conservation law constrained optimization based upon front-tracking*, M2AN Math. Model. Numer. Anal., 40(5), 939–960, 2007.

[23] M. Herty, A. Kurganov, and D. Kurochkin, *Numerical method for optimal control problems governed by nonlinear hyperbolic systems of PDEs*, Commun. Math. Sci., 13(1), 15–48, 2015.

[24] F. James and M. Sepulveda, *Convergence results for the flux identification in a scalar conservation law*, SIAM J. Control Optim., 37(3), 869–891, 1999.
[25] S. Jin and Z.P. Xin, *The relaxation schemes for systems of conservation laws in arbitrary space dimensions*, Commun. Pure Appl. Math., 48(3), 235–276, 1995.
[26] Z. Liu and A. Sandu, *On the properties of discrete adjoints of numerical methods for the advection equation*, Internat. J. Numer. Methods Fluids, 56(7), 769–803, 2008.
[27] A. Bressan and M. Lewicka, *Nonlinear theory of generalized functions*, Shift differentials of maps in BV spaces, Boca Raton, Chapman & Hall/CRC, Boca Raton, FL., 401, 1999.
[28] N.A. Pierce and M. Giles, *Adjoint and defect error bounding and correction for functional estimates*, J. Comput. Phys., 200(2), 769–794, 2004.
[29] S. Ulbrich, *Adjoint-based derivative computations for the optimal control of discontinuous solutions of hyperbolic conservation laws*, System Control Letters, 48, 313–328, 2003.